

# ***A Comprehensive Earthquake Catalog for Iraq in Terms of Moment Magnitude***

**by Tuna Onur, Rengin Gök, Wathiq Abdulnaby, Hanan Mahdi, Nazar M. S. Numan, Haydar Al-Shukri, Ammar M. Shakir, Hussein K. Chlaib, Taher H. Ameen, and Najah A. Abd**

## **ABSTRACT**

A comprehensive earthquake catalog was compiled for Iraq and neighboring areas as part of a broader probabilistic seismic-hazard assessment project. The Iraq Seismic Network (ISN) was established in 1976 and became operational in the early 1980s. However, recording and reporting of seismic data has been intermittent in Iraq. Hence, events were collected from various sources, including the ISN when available, International Seismological Centre (ISC), European-Mediterranean Seismological Centre, U.S. Geological Survey Centennial Catalog, Global Centroid Moment Tensor solutions, and Ambraseys' extensive work on cataloging of instrumental era earthquakes in the Middle East (e.g., Ambraseys, 1978, 2001, 2009). We supplement these with new direct moment magnitude calculations based on coda calibration technique. For many of the larger events in the catalog, more than one magnitude is available. Directly calculated moment magnitudes ( $M_w$ ) were favored, followed by body-wave magnitude ( $m_b$ ) obtained from the ISC. Where no directly calculated  $M_w$  was available, other magnitude scales were converted to  $M_w$  using relationships compatible with the local catalog. The resulting earthquake catalog spans from the year 1900 until the end of 2009, covers the region bounded by 26°–40° N latitudes and 36°–51° E longitudes, and includes more than 18,000 earthquakes, of which roughly 4000 are  $M_w$  4.0 or larger.

*Electronic Supplement:* Earthquake catalog.

## **INTRODUCTION**

Probabilistic seismic-hazard assessments (PSHA) form the basis for most contemporary seismic provisions in building codes around the world. The current building code of Iraq was published in 1997. An update to this edition is in the process of being released. However, there are no national PSHA studies in Iraq to which the new building code can refer for seismic loading in terms of spectral accelerations. As an interim solution, the new draft building code refers to PSHA results produced in

the late 1990s as part of the Global Seismic Hazard Assessment Program (Giardini *et al.*, 1999). These results are (1) more than 15 years outdated and (2) peak ground acceleration-based only (necessitating rough conversion factors to calculate spectral accelerations at 0.3 and 1.0 s for seismic design). Hence, there is a pressing need for a new updated PSHA for Iraq.

Recognizing this need, in 2013 the U.S. Department of Energy through Lawrence Livermore National Laboratory (LLNL) funded a project to engage and train local scientists in Iraq to install new equipment, to improve the quality of seismic monitoring and reporting, and to modernize seismic-hazard mapping efforts in Iraq. In 2014, an initial four-day workshop was conducted in Erbil, Iraq, to present the planning to various participants from Iraqi universities and other research organizations. This workshop was followed by a smaller hands-on workshop at the University of Arkansas at Little Rock, Arkansas. This article presents the results from joint data analysis efforts toward a more robust earthquake catalog for the country.

The starting point for a national PSHA study for Iraq is the establishment of a comprehensive  $M_w$ -based earthquake catalog. The reason why  $M_w$  is the preferred magnitude for the catalog is twofold: (1) almost all contemporary ground-motion prediction equations are in terms of  $M_w$ , and (2)  $M_w$  provides a better quantification of the size of earthquakes, particularly large earthquakes, for which other magnitude scales tend to saturate. Hence, it is important to include direct  $M_w$  calculations to the greatest extent possible, rather than converting from other magnitude scales to  $M_w$ , particularly for large earthquakes.

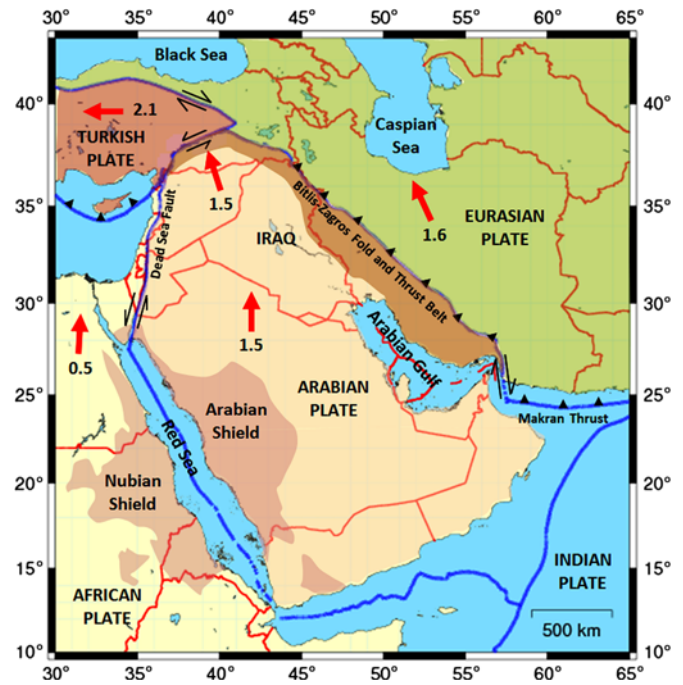
Although global catalogs are available, they are sparse in terms of local earthquakes in this region. For example, the International Seismological Centre-Global Earthquake Model (ISC-GEM) catalog (see [Data and Resources](#)) has 87 earthquakes for our study region (26°–40° N, 36°–51° E) between the years 1900 and 2009 (inclusive) with magnitudes (of various scales) between 5.3 and 7.8 (included in E the electronic supplement to this article). Our compilation includes 237 earthquakes over the same time period and magnitude range.

The most recent regional effort for cataloging earthquakes in terms of  $M_w$  in this area is the Earthquake Model of the Middle East (EMME) project under the auspices of GEM (Zare *et al.*, 2014). Although the EMME catalog is rich in terms of earthquakes in the northern portion of our study area (i.e., areas in eastern Turkey), it is relatively sparse south of the 37.5° N latitude. For example, for 26°–37.5° N latitudes and 36°–51° E longitudes, the Zare *et al.* (2014) catalog includes about 1500  $M_w$  4.0 and larger earthquakes from the year 1900 until the end of 2006 (end of the Zare *et al.*, 2014, catalog). By comparison, our compilation includes ~3500 earthquakes for the same time period, not including contributions from the Zare *et al.* (2014) catalog. Our compilation also includes three additional years of earthquakes, through to the end of 2009, and includes events with magnitudes lower than 4.0, which are not included in the Zare *et al.* (2014) catalog.

Completeness intervals are determined for the catalog described in this article; however, declustering is left to end users because approaches to declustering vary greatly. Earthquake catalogs compiled for PSHA purposes are usually declustered (i.e., dependent events such as fore- and aftershocks are removed from the catalog), leaving a catalog with earthquakes that are independent. This is because most PSHAs are carried out based on the assumption of a Poissonian process, requiring that events happen randomly; that is, occurrence of a given event has no memory of previous event(s). The subset of independent earthquakes remaining in the declustered catalog is therefore intended to be random in time, making the declustered catalog consistent with a Poisson process.

However, there are numerous approaches to declustering for PSHA (e.g., Gardner and Knopoff, 1974; Reasenberg, 1985; Zhuang *et al.*, 2002; Hainzl *et al.*, 2006), and they vary drastically in terms of how many events they identify as independent and dependent events. For example, Zare *et al.* (2014) for their broader study area (11.42°–44.00° N, 30.02°–79.42° E) compare four different declustering methods, leaving anywhere from 7,272 to 24,530 earthquakes in their catalog as independent events out of an initial number of 28,244 earthquakes. There is also debate as to whether declustering should be performed at all (e.g., Boyd, 2012; Marzocchi and Taroni, 2014). Given the wide variation in practices around declustering, we opt to provide an unclustered catalog in this article and leave the decisions around declustering to be made based on the specific needs of each PSHA project.

The resulting catalog described in this article extends geographically between the latitudes of 26° and 40° N and longitudes of 36° and 51° E and temporally between 1900 and 2009 (inclusive). The geographic extent of the catalog's coverage is intended to include sources of seismicity beyond Iraq's borders but which may be damaging inside the territory of Iraq. No minimum magnitude cutoff was used in searches for records in building the catalog. The lowest magnitude in the catalog, before magnitude harmonization, is 0.3, though the catalog is not complete down to this range of magnitude. The full catalog is provided in © Table S1.



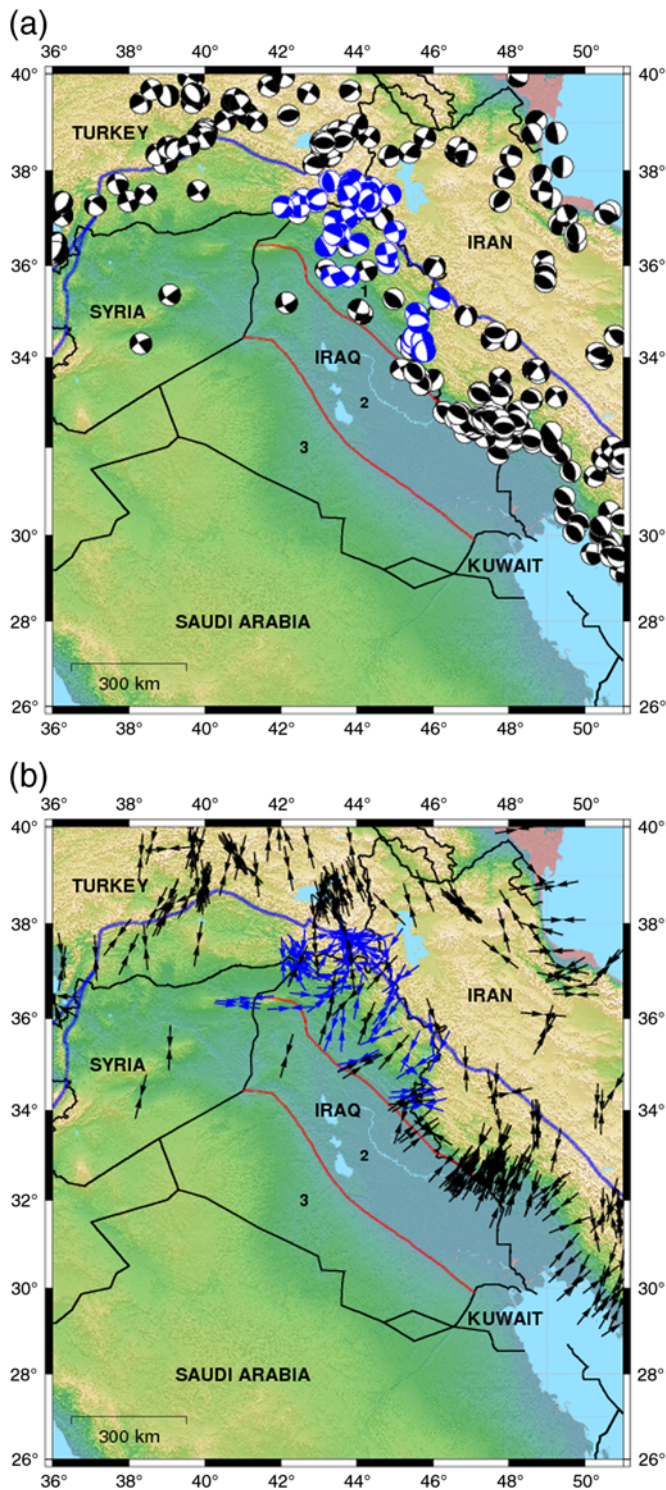
▲ **Figure 1.** Tectonic setting of the region. Thick arrows indicate plate motions in cm/year. The color version of this figure is available only in the electronic edition.

## TECTONIC SETTING OF IRAQ

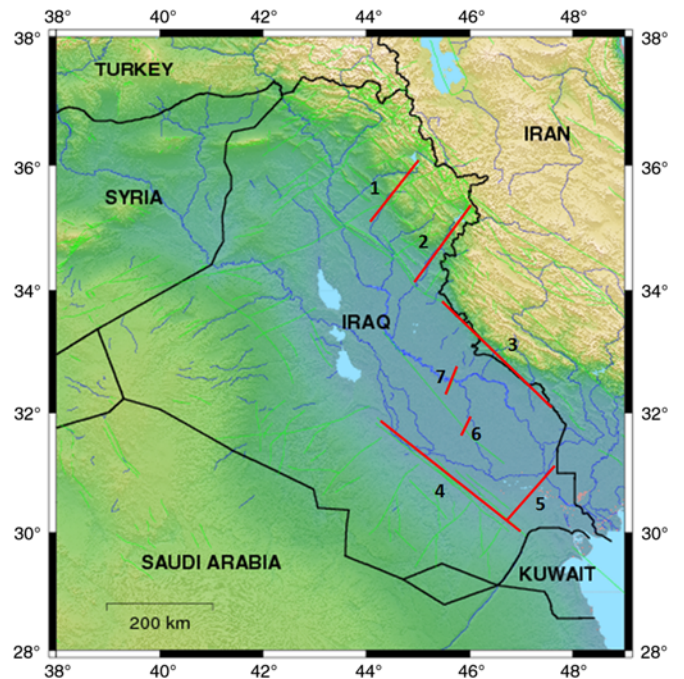
Iraq lies in the northern portion of the Arabian plate (Fig. 1), bounded in the north and east by the Bitlis–Zagros fold-and-thrust belt, where the convergent tectonic boundary between the Eurasian and Arabian plates generates intense earthquake activity. The rest of the country is largely located on the Arabian platform, away from major plate boundaries. The Dead Sea fault system, a major left-lateral transform fault, forms the western boundary of the Arabian platform, about 250 km away from the westernmost part of Iraq.

Iraq is generally divided into three tectonic zones (see e.g., Numan *et al.*, 1998; Fouad and Sissakian, 2011). These divisions, shown in Figure 2, from northeast (NE) to southwest (SW) are (1) the fold-and-thrust zone, (2) the Mesopotamian foredeep, and (3) the inner (stable) Arabian platform.

The Bitlis–Zagros fold-and-thrust belt (zone 1 in Fig. 2) of the Alpine orogen is a seismically active zone (Jackson *et al.*, 1981; Hessami and Jamali, 2006), with intense earthquake activity. Here, the northward-moving Arabian plate is in oblique collision with the Turkish and Iranian plates along the northwest–southeast (NW–SE)-trending suture zone between the colliding plates. The oblique collision results in stress partitioning of the northward stress of the Arabian plate movement into an NE–SW-trending stress perpendicular to the direction of the suture zone and an NW–SE-trending stress parallel to the direction of the suture zone (Numan, 1997). Figure 2b presents stress orientations calculated by Abdunaby *et al.* (2014). In this region, many of the NE–SW-trending (transverse) faults are active, such as the lower Zab fault and the Diyala River fault



▲ **Figure 2.** (a) Focal mechanisms, and (b) stress orientations from [Abdulnaby et al. \(2014\)](#) and Global Centroid Moment Tensor (Global CMT). Tectonic divisions are from [Fouad and Sissakian \(2011\)](#): (1) fold-and-thrust zone, (2) Mesopotamian foredeep, and (3) inner (stable) Arabian platform. The color version of this figure is available only in the electronic edition.



▲ **Figure 3.** Selected active faults in Iraq: (1) lower Zab fault, (2) Diyala River fault, (3) Badra-Amarah fault, (4) Euphrates fault, (5) Hummar fault, (6) Al-Refae fault, and (7) Kut fault. The color version of this figure is available only in the electronic edition.

(marked as 1 and 2 in Fig. 3), as well as the listric (longitudinal) faults that are parallel to the fold axes. According to [Abdulnaby et al. \(2014\)](#), much of the faulting in recent earthquakes is of strike slip, oblique slip, and thrust mechanism (Fig. 2).

The Mesopotamian foredeep (zone 2 in Fig. 2) forms the NE edge of the Arabian platform; however, it differs tectonically from the more stable inner Arabian platform (zone 3 in Fig. 2) to the SW. The Mesopotamian plain contains several buried structures that are evident through their effects on the Quaternary stratigraphy and present geomorphological landforms indicating neotectonic activity of the plain ([Fouad and Sissakian, 2011](#)).

The Quaternary alluvial sediments of the Tigris and Euphrates river systems cover the central and southeastern parts of the Mesopotamian foredeep completely, forming a thick sedimentary sequence ([Sissakian, 2013](#)). The derived seismic models indicate that surface Quaternary sediments thicken southeastward, from 3 km deep in Mosul to 8 km deep in Kuwait ([Gök et al., 2008](#)). The depth of the basement also changes from 8 km ( $\pm 2$  km) within the platform in the west of Iraq to 14 km ( $\pm 2$  km) within the Zagros foreland in the NE and the Mesopotamian plain in the SE ([Numan, 1997](#); [Sissakian, 2013](#)).

Seismically active faults in the Mesopotamian foredeep include the Badra-Amarah fault (along the Iraq–Iran border), Euphrates fault (represents the tectonic boundary between the stable platform and the Mesopotamian foredeep), Hummar fault (north of Basra), Al-Refae fault, and Kut fault. These are faults marked as 3, 4, 5, 6, and 7, respectively, in Figure 3.

The inner Arabian platform (zone 3 in Fig. 2) constitutes a stable tectonic region. Although faults do exist in this zone, recent deformation is much less significant.

It should be noted that, although the stable region is tectonically delineated as zone 3, wave propagation characteristics point to a different demarcation. There is indeed a sharp boundary in the  $S_n$ - and  $L_g$ -wave propagation as the waves move from the Zagros fold-and-thrust belt to the Arabian platform (Al-Damegh *et al.*, 2004), which roughly coincides with the boundary between zones 1 and 2 (Fig. 2).

## MAJOR PREINSTRUMENTAL EARTHQUAKES IN IRAQ

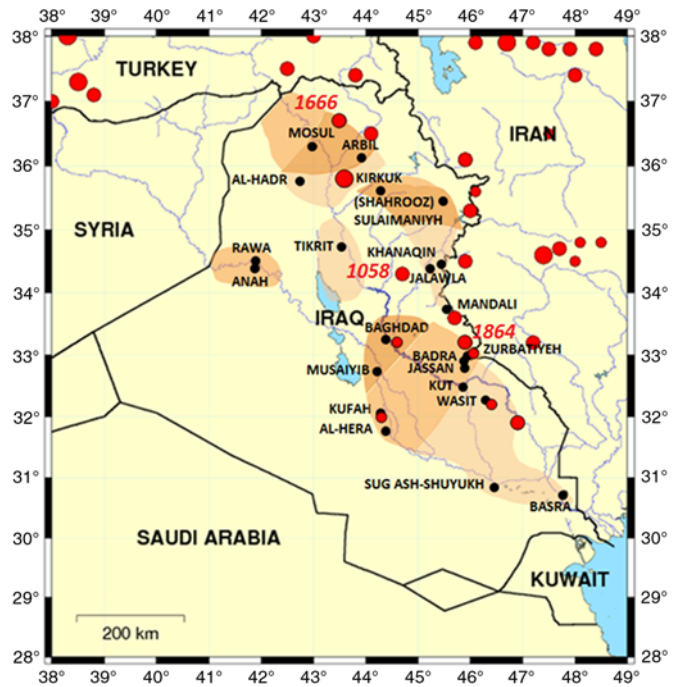
Instrumental earthquake catalogs provide a relatively short snapshot of seismicity of a region, given that the return period of earthquakes is typically longer than the longest instrumental earthquake catalog. To better understand the long-term seismicity (and consequently seismic hazard) in a region, it is imperative to compile any information available on preinstrumental earthquakes: (1) historical earthquakes from written records of past civilizations and (2) prehistorical earthquakes from paleoseismic record. Although this information has limited value in terms of statistical analyses, it provides useful insight as to the locations of potentially damaging future earthquakes.

Information on earthquakes before 1900 in Iraq and neighboring regions can be found in various sources including Alsinawi and Ghalib (1975), various compilations by Ambraseys (e.g., Ambraseys and Melville, 1982; Ambraseys and Jackson, 1998; Ambraseys, 2009), Poirier and Taher (1980), Sbeinati *et al.* (2005), Significant Earthquake Database by the U.S. National Geophysical Data Center (see Data and Resources), and the GEM compilation of historical earthquakes (Albini *et al.*, 2013; Zare *et al.*, 2014). Information on preinstrumental-era earthquakes in Iraq is mainly based on historical written records, such as annals written by early historians. Paleoseismic studies are unfortunately sparse in this region.

Alsinawi and Ghalib (1975) compiled a catalog that includes over 70 events between 1260 B.C. and A.D. 1900, indicating the year of the earthquakes and a description of the impacts, including the names of localities impacted. Ambraseys' compilations provide additional information, such as estimates for magnitudes and locations of the epicenters. Three preinstrumental-era earthquakes that caused significant impact in Iraq are described below. Figure 4 indicates the estimated locations of these earthquakes and presents areas where Alsinawi and Ghalib (1975) report strong earthquake shaking, overlain with historical earthquake epicenters compiled by Ambraseys and Jackson (1998), Albini *et al.* (2013), and Zare *et al.* (2014).

### 8 December 1058 Earthquake of $M_w$ 6.5–7.0 in Eastern Iraq

This earthquake is mentioned in the Annals of the Saljuq Turks: selections from Al-Kamil Fi'l-Ta'rikh of Ibn Al-Athir (Richards, 2014, pp. 128) as follows: "In Shawwal [21 November–19 De-



▲ **Figure 4.** Historical earthquakes in Iraq. Felt-area shading after Alsinawi and Ghalib (1975) for which the darkest shaded areas indicate the most number of earthquakes felt. Small circles indicate  $M_w < 6$ , medium  $6 \leq M_w < 7$ , and large  $M_w \geq 7$ . The estimated epicenters of the 1058, 1666, and 1864 earthquakes are indicated in italics. The color version of this figure is available only in the electronic edition.

ember 1058] there was a great earthquake in Iraq and Mosul. Its effects were felt in Hamadhan. It lasted an hour and destroyed many buildings with large loss of life." Ambraseys and Melville (1982) note the time of this earthquake as 6 p.m. local time on 8 December and estimate its location as western Zagros ( $34.3^\circ$  N,  $44.7^\circ$  E) and its magnitude as 6.4. They also describe that Baghdad was shaken by slow ground movements, causing panic and collapse of many buildings, which resembles a description of surface waves on soft sediments, making earthquake hazard from large distant events a significant concern for the Baghdad area. Poirier and Taher (1980) report the date as 2 December and the intensity of shaking in Mosul as destructive (modified Mercalli intensity [MMI] IX). Shebalin and Tatevossian (1997) estimate the location to be about a degree and a half north and a degree west of the Ambraseys and Melville (1982) estimate and the magnitude to be 7.2 in terms of surface-wave magnitude.

### 22 September 1666 Earthquake of $M_w \sim 7.0$ near Mosul

This earthquake reportedly destroyed five cities and 45 villages in the territory of Mosul and was felt as far away as Armenia, Palestine (Alsinawi and Ghalib, 1975). According to Sbeinati *et al.* (2005), the damage also extended to Sinjar and Sharqat, and the felt area extended to Van (Turkey) and Tabriz (Iran). The location of this earthquake is estimated as  $36.7^\circ$  N,  $43.5^\circ$  E

by [Ambraseys and Jackson \(1998\)](#), and the surface-wave magnitude is estimated to be 6.9 by [Sbeinati \*et al.\* \(2005\)](#) and 7.0 or larger by [Ambraseys and Jackson \(1998\)](#).

### 7 December 1864 Earthquake of $M_w \sim 6.5$ Southeastern Iraq

The exact date for this earthquake is ambiguous. [Ambraseys and Jackson \(1998\)](#) report it to have occurred on 7 December and [Alsinawi and Ghalib \(1975\)](#) on 20 December. It destroyed one village killing 100 people, heavily damaged at least five others, and was strongly felt in Baghdad and Basra ([Alsinawi and Ghalib, 1975](#)). It was followed by a long and strong after-shock sequence that continued until February 1865 ([Alsinawi and Ghalib, 1975](#)), which may be why the date of the main-shock is hard to discern. The location and magnitude are estimated to be 33.2° N, 45.9° E and magnitude 6.4, respectively ([Ambraseys and Jackson, 1998](#)).

## SEISMIC INSTRUMENTATION IN IRAQ

The Department of Geology at the University of Baghdad first started seismic monitoring in Iraq in 1972 using a mobile three-component short-period recording laboratory. In 1976, the Government of Iraq initiated the foundation of a national seismic network (Iraq Seismic Network, ISN). As a result, four short-period stations became operational in the early 1980s: a central station located in Baghdad (BHD) and three secondary stations in Sulaimaniya (SLY), Mosul (MSL), and Rutba (RTB). The Gulf War in 1991 disrupted this network, and half of its stations ceased to operate ([Alsinawi, 2006](#)).

In 2005 two broadband seismic stations were installed, one in Baghdad and one in Mosul with assistance from the University of Arkansas at Little Rock (UALR) and the U.S. Department of Energy. In addition, in August 2005, the North Iraq Seismographic Network was deployed with 10 broadband seismic stations throughout northern, northeastern, and central Iraq. The deployment was coordinated by multiple agencies and sponsored by the U.S. Air Force Research Laboratory ([Gritto \*et al.\*, 2008](#)). In 2008, a small-aperture five-element broadband seismic array (KSIRS) was also added to this network.

In 2007, UALR and LLNL, in collaboration with Duhok University, installed a broadband seismic station in the Duhok area, located in the seismically active fold-and-thrust belt. Seismic data are continuously recorded and archived at this station.

The ISN modernized existing stations and added new equipment in 2009. These are Baghdad (BHD), Mosul (MSL), Rutba (RTB), Nasiriyah (NSR), Badra (IBDR), and Kirkuk (IKRK) stations, all consisting of three-component broadband seismometers.

In 2014, a seven-element high-frequency three-component array was installed by UALR and LLNL, in collaboration with the University of Thi-Qar, in the Al-Refaee area, located in the Mesopotamian foredeep. Although this area experienced swarms of moderate-size felt earthquakes in 2004 and 2013, many of these earthquakes were not recorded, due to lack of

instrumentation nearby. The purpose of this array was to better locate earthquakes in this region and to locate these swarms with enough accuracy to map any active faults that may be generating these earthquakes.

Five other broadband seismic stations were installed in 2014 and 2015 by UALR and LLNL, in collaboration with University of Baghdad, University of Thi-Qar, University of Basra, and University of Sulaimani. These five stations were installed in Nasiriyah, Basra, Ammarah, Sulaimaniya, and Karbala. Seismic data are continuously recorded and archived at these stations. Two strong-motion stations were also installed as part of this effort in Basra and Sulaimaniya.

## INSTRUMENTAL EARTHQUAKE CATALOG

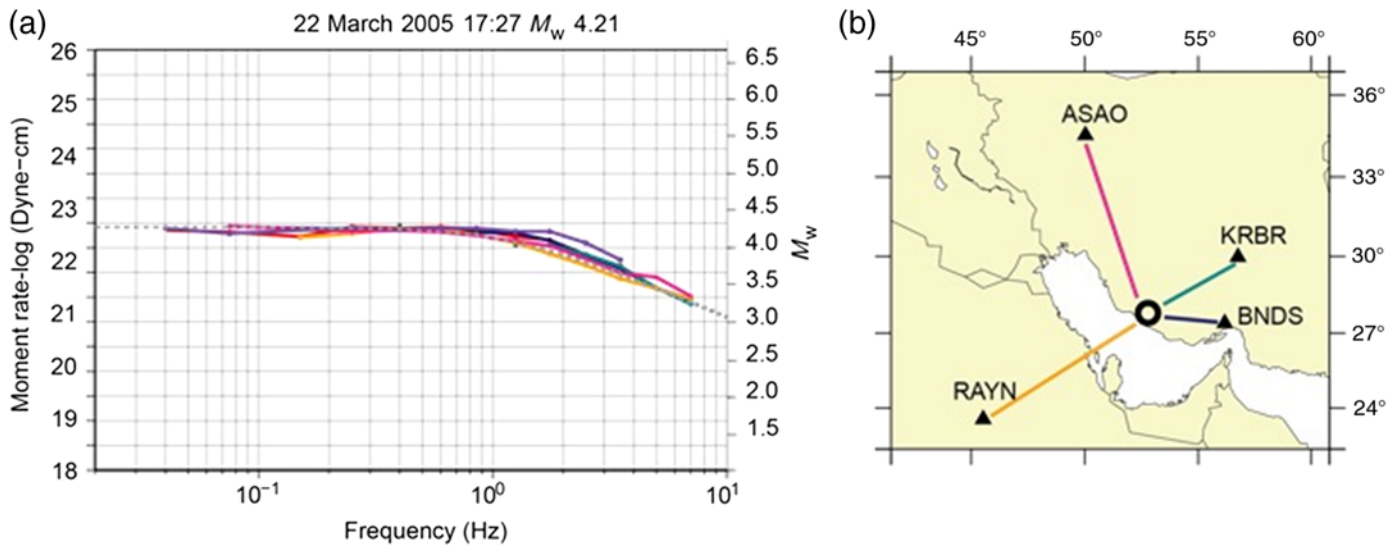
The instrumental catalog described in this article uses the ISC Bulletin as a base (see [Data and Resources](#)) for the region between 36°–51° E longitudes and 26°–40° N latitudes. Only the Reviewed ISC Bulletin is used, which is typically 24 months behind real time. The base catalog is further supplemented by the following sources: the pre-1964 portion of the catalog is supplemented by [Fahmi and Al Abbasi \(1989\)](#), [Ambraseys \(2001\)](#), [Zare \*et al.\* \(2014\)](#), [Riad and Meyers \(1985\)](#), and U.S. Geological Survey (USGS) Centennial ([Engdahl and Villaseñor, 2002](#)) catalogs. These five sources identify a significant number of early events (between 1900 and 1964) that are not listed in the ISC Bulletin.

The USGS Centennial catalog (see [Data and Resources](#)) is a compilation of large earthquakes in which all available magnitudes for each earthquake in the catalog were reviewed to provide a reliable magnitude. It is considered to be complete down to magnitude 5.5 from 1964, to magnitude 6.5 from the 1930s, and to magnitude 7.0 from 1900.

The post-1976 portion of the catalog is supplemented by the Global Centroid Moment Tensor (Global CMT) solutions (see [Data and Resources](#)), which provides  $M_w$  calculations using the [Kanamori \(1977\)](#) formulation for moderate-to-large earthquakes globally. It should be noted that, for a small number of earthquakes, searches conducted after 1 February 2006 will give values for  $M_w$  that differ by 0.1 magnitude unit from values given by searches prior to that date, due to a rounding procedure that was used prior to 1 February 2006. The catalog described in this article uses values as calculated after 1 February 2006.

Post-1989, a portion of the catalog is supplemented by  $M_w$  calculated by a coda calibration technique. This is a new dataset that provides moment magnitudes for nearly 1000 earthquakes of  $M_w > 2.5$ , significantly adding to the number of directly calculated  $M_w$  in this magnitude range. The coda calibration method used for these calculations is described further in the [M<sub>w</sub> Calculations Using the Coda Calibration Technique](#) section.

Post-1998, a portion of the catalog is supplemented by the European-Mediterranean Seismological Centre data published as the Euro-Med Bulletin (see [Data and Resources](#)). The Euro-Med Bulletin includes data from the ISN; however, it should be noted that reporting from the ISN has been sporadic. The



▲ **Figure 5.** (a) Example source spectra shown with (b) various stations in the Middle East. The dotted line is theoretical spectra for  $M_w$  4.21. The scatter is significantly low due to coda averaging effect (Gök *et al.*, 2016). The color version of this figure is available only in the electronic edition.

Euro-Med Bulletin contributes significantly to the small-magnitude completeness in recent years. For example, of the roughly 2500 earthquakes in the year 2007, about 1000 are in the Euro-Med Bulletin but not in the ISC Bulletin. The trend is similar for 2008 (almost half of roughly 2400 earthquakes) and 2009 (more than half of roughly 3200 earthquakes).

The Euro-Med Bulletin is roughly three years behind real time. At the time we began our compilation, it was available until the end of 2009. Because of its significant contribution to small-magnitude earthquakes, our compilation is truncated to the same date.

Post-2005, a portion of the catalog is supplemented by Abdulnaby *et al.* (2014), which provides moment magnitudes calculated by the waveform moment tensor inversion method for 65 events of magnitude greater than or equal to 3.3 in northern and northeastern Iraq from 2004 until 2013. The seismic data used for these calculations were obtained from 54 broadband stations that belong to the Kandilli Observatory and Earthquake Research Institute (KOERI), the Incorporated Research Institutions for Seismology, the Observatories and Research Facilities for European Seismology, the ISN, and the Duhok station installed by UALR and LLNL (Abdulnaby *et al.*, 2013, 2014).

The resulting catalog encompasses the region between 36°–51° E longitudes and 26°–40° N latitudes and includes about 16,000 events of magnitude 3.0 and larger and about 4000 events of magnitude 4.0 and larger between the years 1900 and 2009 inclusive.

## $M_w$ CALCULATIONS USING THE CODA CALIBRATION TECHNIQUE

Calculation of moment magnitudes of moderate-to-small-size events is a challenge using traditional methods (e.g., waveform

modeling and spectral fitting). It has been shown that regional moment tensor inversion methods can introduce a bias, due to velocity structure effect on higher frequencies for smaller-size events. If the structure is not known well, the regional moment tensor solutions will either underestimate or overestimate up to half of the magnitude units, and it may be higher in some extreme cases. To avoid these biases, we use the coda calibration method (Mayeda *et al.*, 2003; Gök *et al.*, 2016) to obtain moment magnitudes. Robustness and unbiased estimate of the  $M_w$  using coda technique has been shown in various parts of the world (e.g., Italy by Morasca *et al.*, 2005, and Turkey by Eken *et al.*, 2004; Gök *et al.*, 2009).

The method is described in detail at Mayeda *et al.* (2003) and Gök *et al.* (2016). First, the coda amplitudes are measured at 13 narrow frequency bands (between 0.02 and 8 Hz) to obtain source spectra at each station (Fig. 5). After all the amplitudes are collected from all the stations at 13 frequency bands, a simple empirical technique is used to correct for path and geometrical spreading effects. These empirical corrections are then applied to the coda amplitudes in each frequency to obtain dimensionless amplitudes. The next step is to tie these to known  $M_w$  measurements calculated in the region through independent techniques such as 1D long-period waveform modeling. We use seismic moment estimates from two independent studies for this purpose: (1) from Gene Ichinose (personal comm., 2015), who uses waveform inversions with a velocity model specific to the region, and (2) Covellone and Savage (2012), who use an adjoint method, in which they improve the model during moment tensor inversion. Comparison of common events obtained using both techniques to examine any bias showed that the  $M_w$ s were consistent, with no bias and relatively small scatter. Hence, once the correction is applied at each frequency, all the measured envelopes provided moment

**Table 1**  
Distribution of  $M_w$  by Source for Earthquakes of Magnitude  $\leq 5$  with Direct  $M_w$  Calculations

$M_w$ Source	1989–2009*
Direct $M_w$ (Global CMT)	20
Direct $M_w$ (this article)	1081
Direct $M_w$ (other sources) <sup>†</sup>	61
Total	1162

\*No direct  $M_w$  is available at this magnitude range prior to 1989.  
<sup>†</sup>Other sources include International Seismological Centre (ISC), European-Mediterranean Seismological Centre (EMSC), and [Abdulnaby et al. \(2014\)](#).

magnitudes for roughly 1000 events ( $M_w > 2.5$ ) that fall inside our catalog region.

In our study region, the Global CMT generally gives higher  $M_w$  than the coda calibration technique by about 0.1 magnitude unit in the 4.5–6.5 magnitude range. In this study, we generally use the coda-based solutions for magnitudes between 3.0 and 5.0 (Table 1). The moment magnitudes ( $M_w$ ) obtained from the coda technique are used both as direct  $M_w$  estimations for the catalog and to find relationships between  $M_w$  and other magnitude scales ( $M_D$ ,  $M_L$ , and  $m_b$ ).

## CATALOG MERGING

Earthquake data including date, time, location, depth, and magnitude from the seven different sources described above have been collected and merged to form a comprehensive instrumental catalog of earthquakes for Iraq and neighboring regions. As part of the merging of catalogs, duplicate earthquakes are identified based on the location and time of the earthquake, and lower priority entries are removed from the catalog.

Different prioritization schemes are applied for location and magnitude. Because the ISC Bulletin uses data contributed by various seismological agencies from around the world to locate earthquakes, its locations are generally used as the basis for this compilation. For those earthquakes that are not included in the ISC Bulletin, the location solution provided by the agency from which the earthquake information was obtained is used.

In terms of magnitudes, direct moment magnitude ( $M_w$ ) assignments are favored in this compilation, followed by ISC body-wave magnitude ( $m_b$ ) assignments. If  $M_w$  is available from more than one agency, the Global CMT solution is favored. Out of roughly 200 post-1964 earthquakes with a magnitude larger than 5.0, about 140 have a direct  $M_w$  assignment. This ratio increases to 135 out of about 165 for the post-1976 period, when the Global CMT catalog starts (Table 2).

## MAGNITUDE HARMONIZATION

Because the purpose of this study is to prepare a catalog in terms of  $M_w$ , the next step is the harmonization of magnitude

**Table 2**  
Distribution of  $M_w$  by Time and Source for Earthquakes of Magnitude  $> 5$

$M_w$ Source	1965–1975	1976–1988	1989–2009
Direct $M_w$ (AMB)*	6	—	—
Direct $M_w$ (Global CMT)	N/A	32	82
Direct $M_w$ (this article)	N/A	N/A	21
$M_w$ converted from $m_b$	28	20	8
$M_w$ converted from $M_L$	—	—	1
Total	34	52	112

\*AMB, various Ambraseys compilations (e.g., [Ambraseys, 2001](#)).

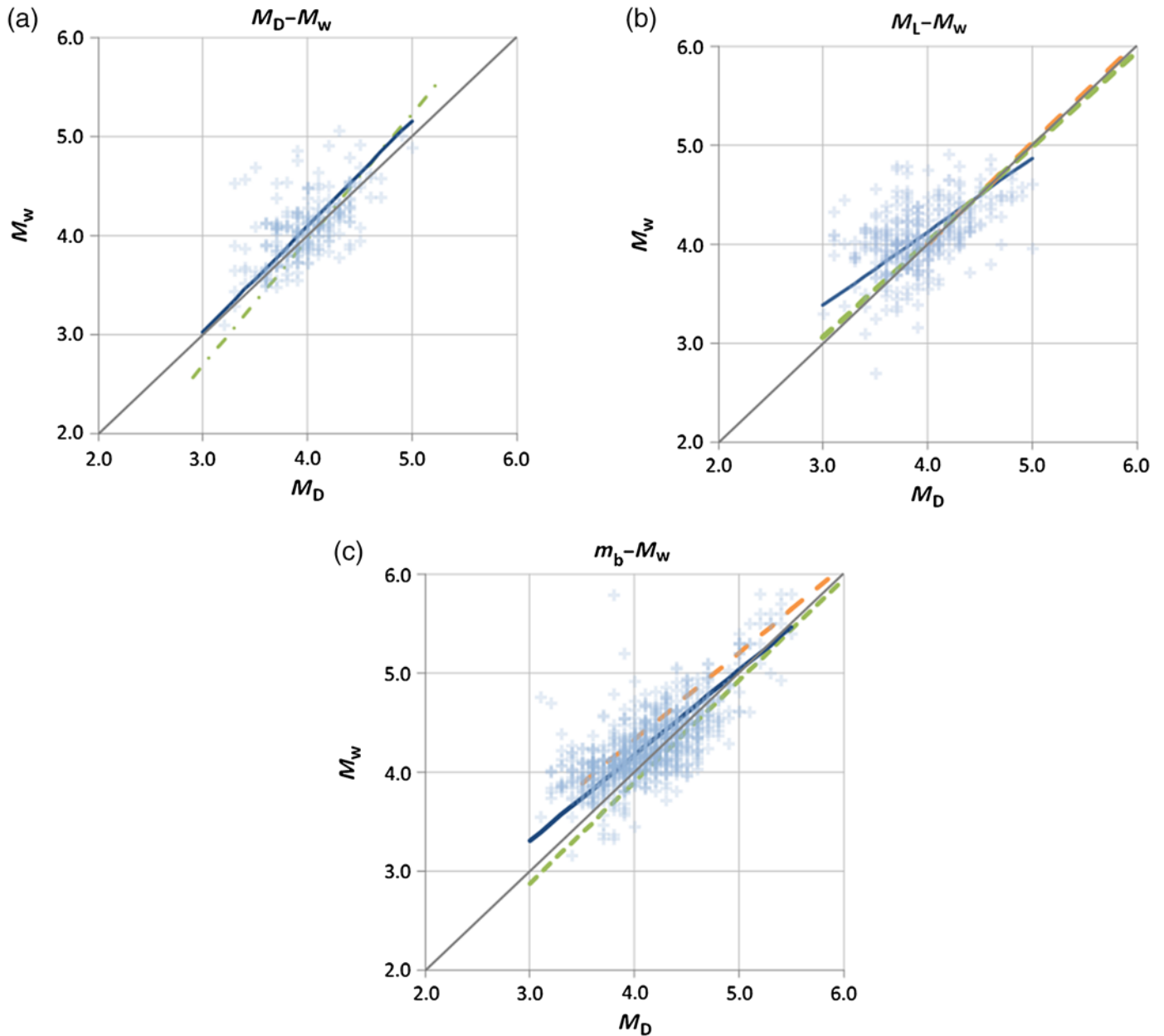
scales. Once the merging, clean up, and magnitude prioritization are applied, the majority of the smaller earthquakes (magnitude  $< 5$ ) in the resulting catalog are in terms of  $M_D$  (about three-fifth),  $M_L$  (about a fifth), or  $m_b$  (about an eighth) magnitude scales (Table 3). Hence,  $M_D$ – $M_w$ ,  $M_L$ – $M_w$ , and  $m_b$ – $M_w$  relationships are needed.

To develop these relationships, we use the entries in our catalog in which multiple magnitudes are reported for the same event. Instead of a least-squares fit to the data, which requires that the uncertainty on the independent variable (i.e.,  $M_D$ ,  $M_L$ , and  $m_b$ ) is at least one order of magnitude smaller than the one on the dependent variable (i.e.,  $M_w$ ), we utilize orthogonal regression, which allows both the dependent and independent variables to be affected by uncertainty ([Castellaro et al., 2006](#)). Consequently, instead of minimizing the sum of square differences between a dependent variable and its empirical estimation (ordinary least squares), we minimize the sum of square distances from each set of points to the regression line (orthogonal regression) to obtain regression coefficients for each magnitude conversion relation. Further discussion, detailed formulation, and examples for orthogonal regression can be found in [Kendall and Stuart \(1979\)](#), [Castellaro et al. \(2006\)](#), and [Deniz and Yucemen \(2010\)](#).

Because a significant proportion of  $M_D$  assignments is contributed by the agency ISK (KOERI, Istanbul, Turkey), these are used in the  $M_w$ – $M_D$  regression. Generally for post-1965 earthquakes of magnitude  $> 5$ , direct  $M_w$  calcula-

**Table 3**  
Magnitude Types in the Catalog before Harmonization

Magnitude Type	Number	Time Period	Magnitude Range
$M_D$	10,771	1992–2009	0.2–5.0
$M_L$	3,012	1982–2009	0.5–5.4
$m_b$	2,200	1964–2009	2.5–5.6
$M_w$	1,333	1900–2009	2.2–7.7
$M_c$	197	1999–2009	0.3–4.4
$M_s$ , $M_{pv}$ , $M_n$ , and $M_G$	< 20	1992–2007	2.5–4.5



▲ **Figure 6.** (a) Comparison of  $M_D$  from ISK to the coda-based  $M_w$  from this study. The solid line is an orthogonal regression fit to the data (equation 1), the dashed-dotted line is the  $M_D$ – $M_w$  relationship by Deniz and Yucemen (2010). (b) Comparison of  $M_L$  from various agencies and coda-based  $M_w$  from this study. The solid line is an orthogonal regression fit to the data (equation 2), the short-dashed line is the  $M_L$ – $M_w$  relationship by Gök *et al.* (2016), and the long-dashed line by Zare *et al.* (2014). (c) Comparison of  $m_b$  from International Seismological Centre to the  $M_w$  from Global CMT and coda-based  $M_w$  from this study. The solid line is an orthogonal regression fit to the data (equation 3), the short-dashed line is the  $m_b$ – $M_w$  relationship by Gök *et al.* (2016), and the long-dashed line by Zare *et al.* (2014). The color version of this figure is available only in the electronic edition.

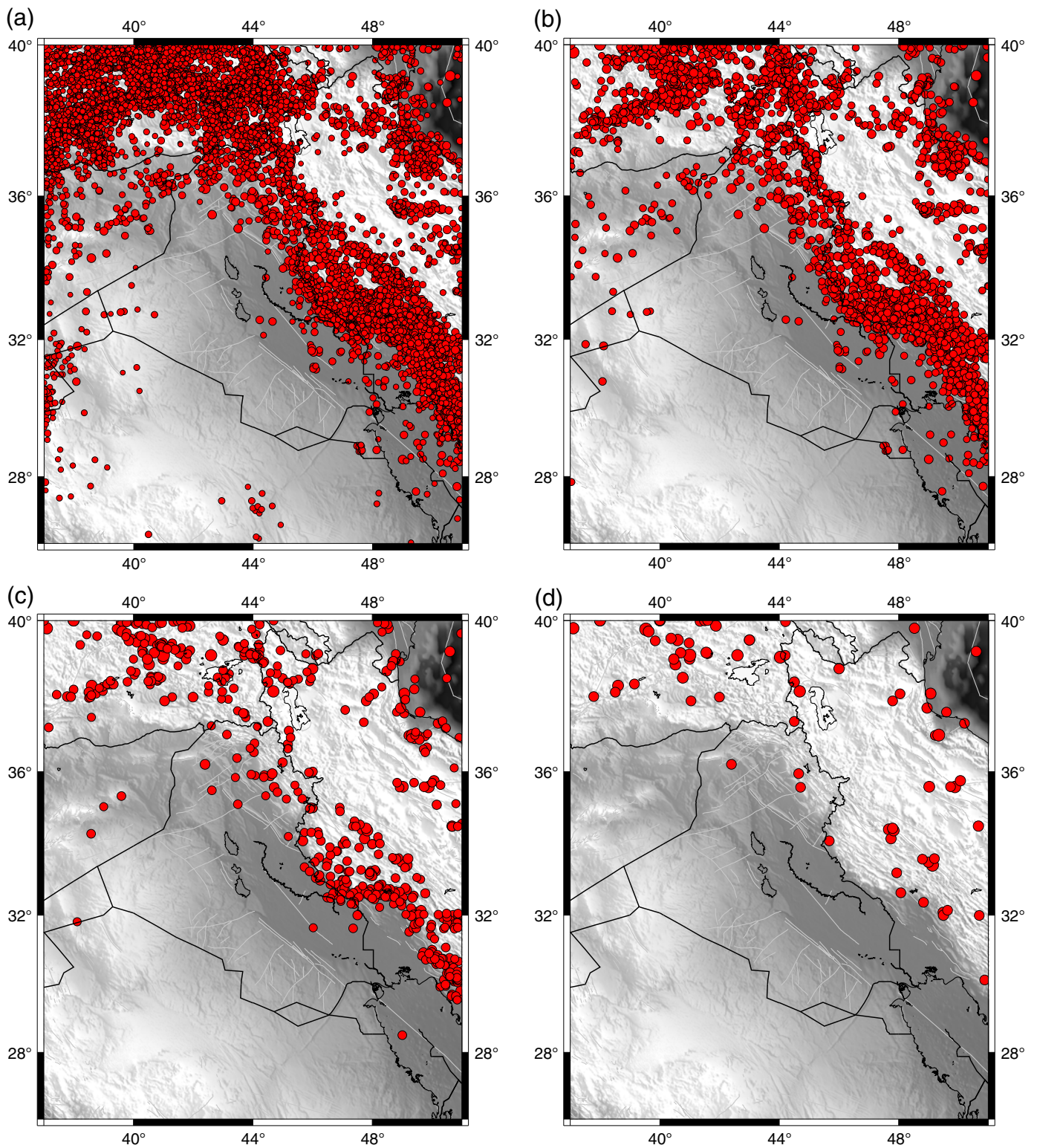
tions are available. Hence, the focus of the comparison is on earthquakes of magnitude between 3 and 5. Because most of the directly calculated  $M_w$  at this magnitude range are those from coda calibration method described above (Table 1), we use these for the  $M_w$ – $M_D$  regression.

The data from over 200 earthquakes for which both ISK  $M_D$  and coda  $M_w$  are available are shown in Figure 6a, and the relationship obtained from orthogonal regression is given in

equation (1) along with the magnitude range for which the relationship is valid and the number of data points used for the regression. A relationship developed by Deniz and Yucemen (2010) based on Turkish data, which is similar to our regression, is also plotted in Figure 6a.

$$M_w = 1.067 \times M_D + 0.1758, \quad 3.0 < M_D < 5.0, \\ R^2 = 0.63, \quad n = 223. \quad (1)$$

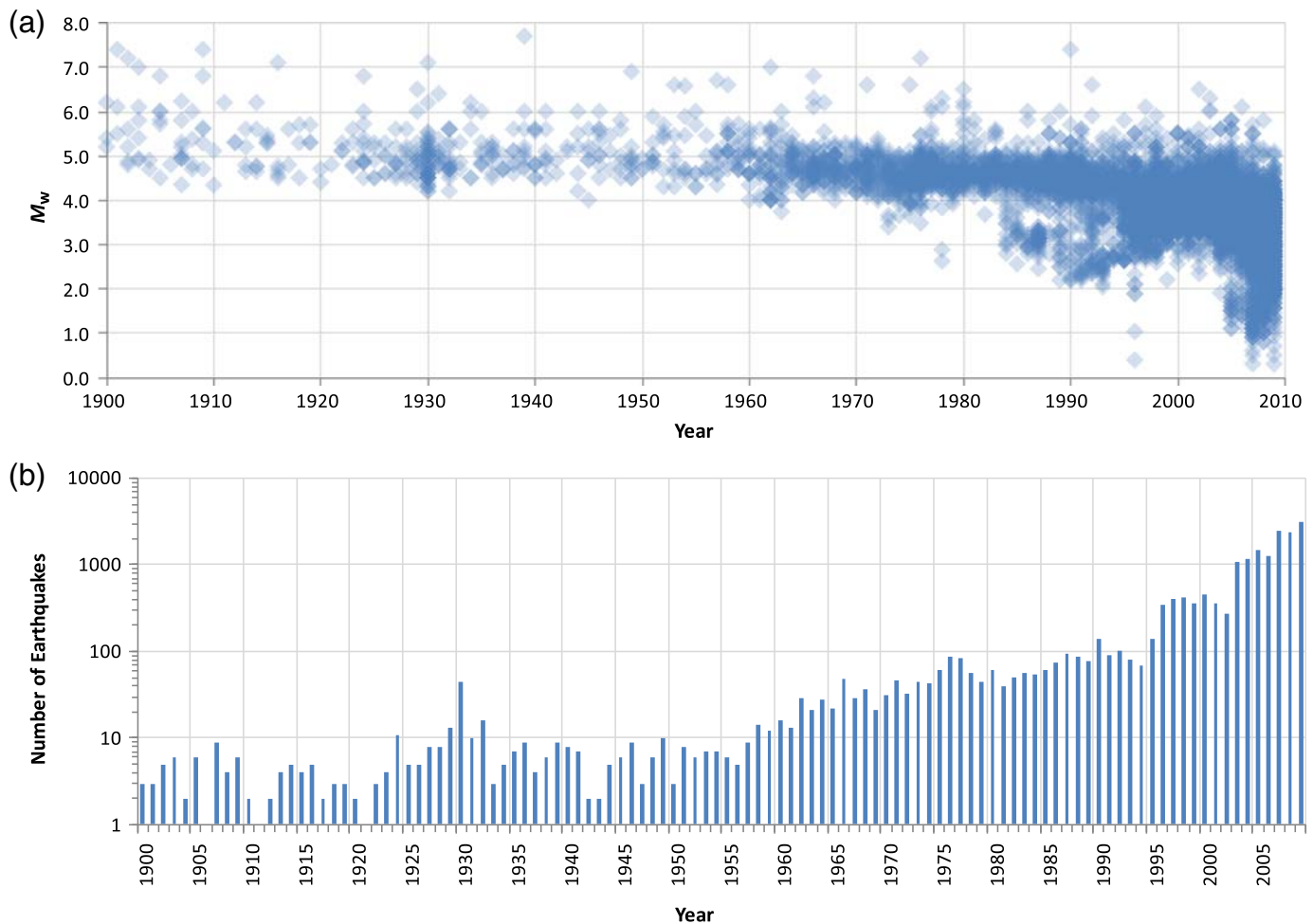




▲ **Figure 7.** Spatial distribution of earthquakes in the harmonized catalog: (a)  $M_w > 3$ , (b)  $M_w > 4$ , (c)  $M_w > 5$ , and (d)  $M_w > 6$ . The color version of this figure is available only in the electronic edition.

A comparison of  $M_L$  to  $M_w$  in the magnitude 3–5 range is presented in Figure 6b. In this case,  $M_L$  is obtained from various agencies instead of a single agency because the data are not dominated by single agency, as in the case of  $M_D$ . The relation-

ship derived here uses over 300 earthquakes (equation 2) for which both  $M_w$  and  $M_L$  values are available in the catalog. Two relationships derived from broader regions that include our study area are also plotted in Figure 6b. The short-dashed



▲ **Figure 8.** (a) Temporal distribution of earthquakes in the harmonized catalog. (b) Number of earthquakes in the harmonized catalog by year. The color version of this figure is available only in the electronic edition.

line is the relationship by [Gök \*et al.\* \(2016\)](#) and the long-dashed line is by [Zare \*et al.\* \(2014\)](#). Both are close to each other and the 1:1 line and differ slightly from this study. The range of magnitudes for the [Zare \*et al.\* \(2014\)](#)  $M_L$ - $M_w$  relationship is limited to  $M_L \geq 4.0$ .

$$M_w = 0.7441 \times M_L + 1.147, \quad 3.0 < M_L < 5.0, \\ R^2 = 0.39, \quad n = 323. \quad (2)$$

Finally, a comparison of  $m_b$  to  $M_w$  is presented in Figure 6c. In this case, the magnitude range is extended to about 5.5 because of the significant number of entries with only  $m_b$  assignments in this magnitude range. Because a large majority of the  $m_b$  is provided by the ISC, and our priority scheme among  $m_b$  has ISC as the highest priority, we plot ISC  $m_b$  only. On the other hand, both coda-based (dominating the magnitude  $< 5$  range) and Global CMT (dominating the magnitude  $> 5$  range)  $M_w$  were used in the comparison. The  $m_b$ - $M_w$  relationship, derived using an orthogonal fit to about 800 data points, is presented in equation (3) and Figure 6c. The relationships by [Gök \*et al.\* \(2016\)](#) and [Zare \*et al.\* \(2014\)](#) are also plotted in Figure 6c.

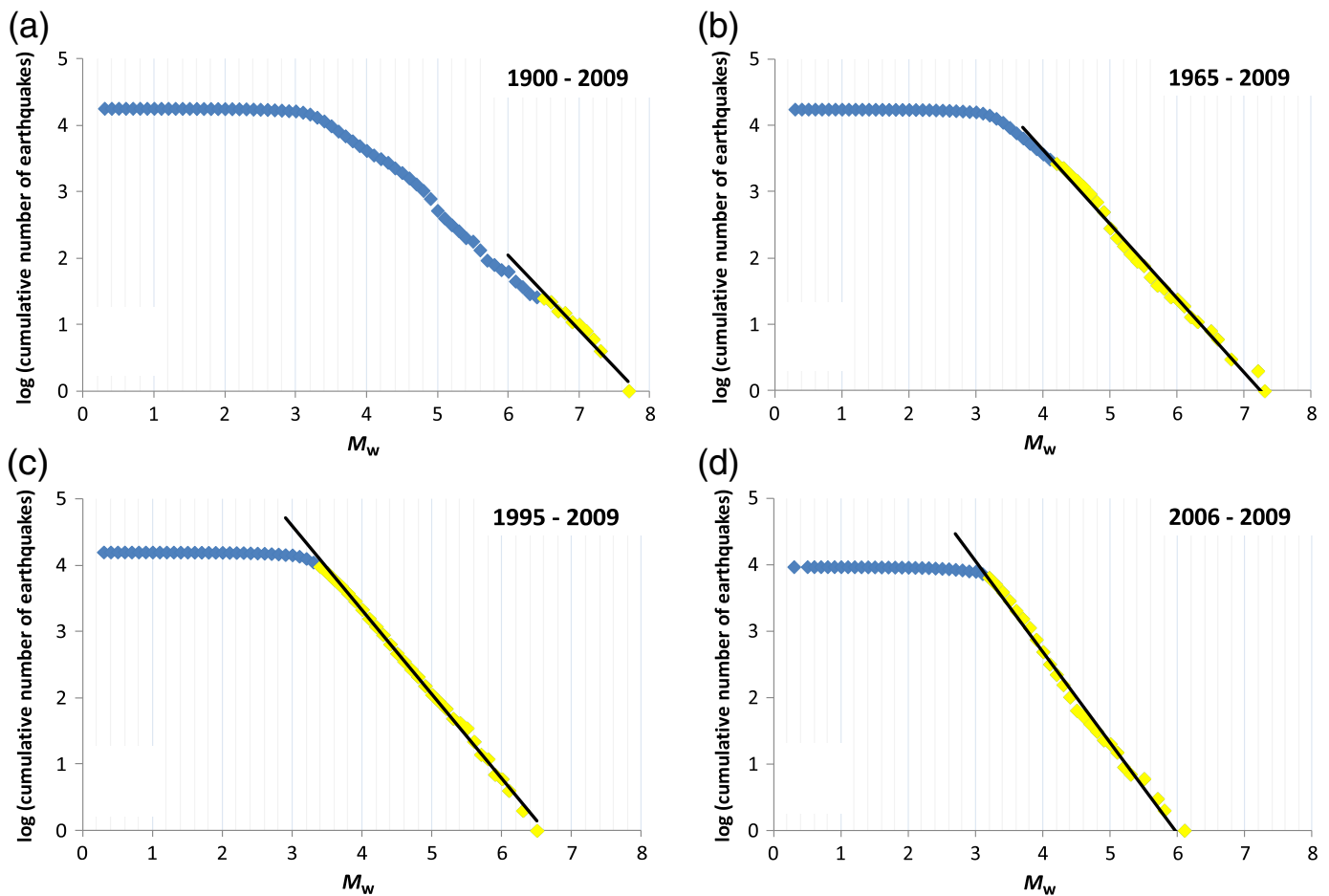
The range of magnitudes for the [Zare \*et al.\* \(2014\)](#)  $m_b$ - $M_w$  relationship is limited to  $m_b \geq 3.5$ .

$$M_w = 0.8599 \times m_b + 0.7278, \quad 3.0 < m_b < 5.5, \\ R^2 = 0.69, \quad n = 792. \quad (3)$$

Less than 2% of the earthquakes in our catalog have magnitude scales other than  $M_w$ ,  $M_D$ ,  $M_L$ , or  $m_b$  because they only have magnitude entries such as  $M_c$ ,  $M_{pv}$ ,  $M_G$ , and  $M_n$ . Because of their small number, it was not feasible to do a statistically significant regression between these magnitude scales and  $M_w$ . The magnitudes of these few earthquakes are assumed to be equivalent to  $M_w$ , in the absence of a more suitable solution. Though a large number of earthquakes also have  $M_s$  assignments, almost all those events have either  $M_w$  or  $m_b$  available; hence, an  $M_s$ - $M_w$  relationship was not utilized in this study.

The depth distribution of the earthquakes in the catalog exhibits mainly shallow crustal seismic activity. About 91% of the earthquakes have a depth between 0 and 35 km.

The resulting catalog with magnitudes harmonized to  $M_w$  is plotted in Figure 7. Although the intense seismicity is mainly



▲ **Figure 9.** Cumulative rate of earthquakes by magnitude for selected time periods: (a) 1900–2009, (b) 1965–2009, (c) 1995–2009, and (d) 2006–2009. The color version of this figure is available only in the electronic edition.

concentrated along the Bitlis–Zagros fold-and-thrust belt, earthquakes also occur in other parts of the country. The quietest in terms of seismic activity are the central and southern areas of Iraq, deeper into the Arabian platform.

## CATALOG COMPLETENESS

Completeness intervals indicate the lowest magnitude at which all earthquakes are deemed to be included in the catalog. Catalog completeness is an essential component of seismic activity studies. Without the appropriate completeness intervals, recurrence parameters calculated from the catalog would be biased.

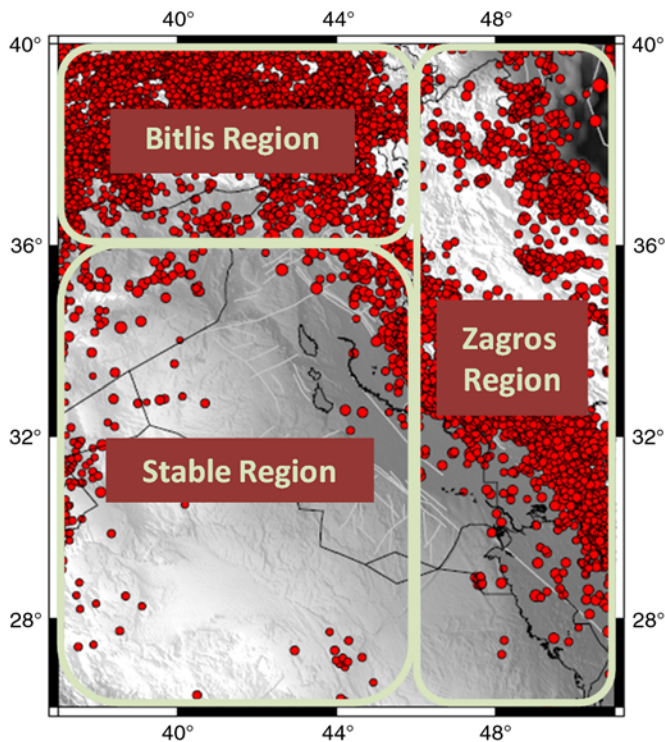
The distribution of earthquakes over time for the harmonized catalog compiled in this study is plotted in Figures 8a by magnitude and in Figure 8b by number. Broadly, the catalog goes down to magnitude 5.5 starting in 1920s, magnitude 4 starting mid-1960s, magnitude 3 starting mid-1990s, and magnitude 2.5 starting mid-2000s. These dates generally coincide with increase in seismic instrumentation globally such as at the end of World War I (1918), the WWSSN becoming operational (mid-1960s), and activation of the Comprehensive Nuclear-Test-Ban Treaty Organization (mid-1990s). Locally, the data availability significantly increases after 2005.

Completeness intervals for the catalog are derived from plots of the logarithm of cumulative rate of earthquakes against magnitude (Fig. 9), prepared for various time periods and by noting at which magnitude the slope of the curve deviates from a straight line. The resulting completeness intervals for the entire catalog are as follows:  $M_w$  6.5 and above are complete since 1900,  $M_w$  6.0 and above since 1924,  $M_w$  4.2 and above since 1965,  $M_w$  3.4 and above since 1995, and  $M_w$  3.2 and above since 2006.

However, completeness intervals are also region dependent. To capture the regional variability, we divide the catalog into three broad regions (Fig. 10), based on a detailed region-by-region analysis, and evaluate completeness intervals for each region: (1) Bitlis region, (2) Zagros region, and (3) stable region. The resulting region-dependent completeness intervals are presented in Table 4.

## RESULTS AND CONCLUSIONS

A comprehensive earthquake catalog in terms of  $M_w$  is developed for Iraq. The new catalog fills a gap in this region by focusing particularly on the territory of Iraq where instrumentation and earthquake reporting has been intermittent. Existing





▲ **Figure 10.** Catalog completeness regions. The color version of this figure is available only in the electronic edition.

global and regional catalogs are merged, duplicate earthquakes cleaned, and the resulting catalog is supplemented by direct moment magnitude calculations for Iraq, using coda calibration technique and moment tensor solutions.


Regional magnitude conversion relations are developed to convert three magnitude scales that are dominant in the catalog ( $M_D$ ,  $M_L$ , and  $m_b$ ) to  $M_w$ , in which direct  $M_w$  calculations are unavailable. General orthogonal regression is used for developing the relations because it allows the uncertainty in both the dependent and independent variables to be of a similar order of magnitude. The  $M_D$ - $M_w$  and  $M_L$ - $M_w$  relations developed are valid between magnitudes 3.0 and 5.0, and the  $m_b$ - $M_w$  relations are valid between magnitudes 3.0 and 5.5. The relations developed in this study differ noticeably but not drastically from other relations developed for this region.

The catalog presented in this article extends between the latitudes of 26° and 40° N and longitudes of 36° and 51° E. Although the current time period covered is from 1900 until the end of 2009, the catalog will be regularly updated and will be made available online.

The current version of the catalog is provided as an  electronic supplement to this article. The completeness intervals are  $M_w$  6.5 and above since 1900,  $M_w$  6.0 and above since 1924,  $M_w$  4.2 and above since 1965,  $M_w$  3.4 and above since 1995, and  $M_w$  3.2 and above since 2006. However, as noted earlier, completeness varies by region. The catalog provided in  Table S1 is the full catalog, and application of the completeness intervals is left to users.

This catalog is intended to enable a much-needed update to hazard assessments in the country so as to provide the basis for strengthened seismic provisions in the upcoming building code update. Iraq's earthquake monitoring capability has been gradually improving since 2005, which allows (1) improvements in completeness of the catalog at small magnitudes, and (2) moment magnitudes to be routinely calculated going forward, reducing the need to convert from other magnitude scales.

## DATA AND RESOURCES

The data used in this article can be found at the following websites: European-Mediterranean Seismological Centre (EMSC), available at <http://www.emsc-csem.org/Bulletin/> (last accessed July 2015); Global Centroid Moment Tensor (Global CMT) solutions, available at <http://www.globalcmt.org/CMTsearch.html> (last accessed July 2015); Global Earthquake Model (GEM), available at <http://www.globalquakemodel.org/> (last accessed February 2016); International Seismological Centre Bulletin (ISC), available at <http://www.isc.ac.uk/iscbulletin/> (last accessed July 2015); International Seismological Centre (ISC-GEM) Global Instrumental Catalogue, v.2.0, released on 19 January 2015, available at <http://www.isc.ac.uk/iscgem/> (last accessed on July 2015); U.S. National Geophysical Data Center (NGDC/WDS), available at <http://www.ngdc.noaa.gov/nndc/struts/form?t=101650&s=1&d=1> (last accessed February 2016); and the U.S. Geological Survey (USGS) Centennial Catalog, available at <http://earthquake.usgs.gov/data/centennial/> (last accessed July 2015). 

## ACKNOWLEDGMENTS

This work benefited greatly from discussions in two different workshops, one in Erbil, Iraq, in June 2014, and a smaller one in Little Rock, Arkansas, in April 2015. We are grateful to more than 30 attendees of the Iraq workshop for their enthusiasm to attend the workshop under difficult circumstances and for their contributions to this effort. We also appreciate

**Table 4**  
**Regional Variation of Completeness Intervals**

Region	1900–2009	1924–2009	1965–2009	1995–2009	2006–2009
Bitlis ( $M_w$ )	6.5+	5.5+	3.4+	3.2+	3.2+
Zagros ( $M_w$ )	6.5+	6.0+	4.5+	4.3+	3.8+
Stable ( $M_w$ )	6.5+	6.0+	4.5+	3.4+	3.4+

the energy and hard work the participants brought into the second workshop, giving us great input and feedback and helping move this project forward. This work was performed under the auspices of the U.S. Department of Energy by Lawrence Livermore National Laboratory (LLNL) under Contract Number DE-AC52-07NA27344. This is LLNL Contribution Number LLNL-JRNL-682738.

## REFERENCES

- Abdulnaby, W., H. Mahdi, H. Al-Shukri, and N. M. S. Numan (2014). Stress patterns in Northern Iraq and surrounding regions from formal stress inversion of earthquake focal mechanism solutions, *Pure Appl. Geophys.* **171**, no. 9, doi: [10.1007/s00024-014-0823-x](https://doi.org/10.1007/s00024-014-0823-x).
- Abdulnaby, W., H. Mahdi, N. M. S. Numan, and H. Al-Shukri (2013). Seismotectonics of the Bitlis–Zagros fold and thrust belt in northern Iraq and surrounding regions from moment tensor analysis, *Pure Appl. Geophys.* **171**, no. 7, doi: [10.1007/s00024-013-0688-4](https://doi.org/10.1007/s00024-013-0688-4).
- Albini, P., R. M. W. Musson, A. A. Gomez Capera, M. Locati, A. Rovida, M. Stucchi, and D. Viganò (2013). Global historical earthquake archive and catalogue (1000–1903), *GEM Technical Report 2013-01 V1.0.0*, GEM Foundation, Pavia, Italy, 202 pp., doi: [10.13117/GEM.GEGD.TR2013.01](https://doi.org/10.13117/GEM.GEGD.TR2013.01).
- Al-Damegh, K., E. Sandvol, A. Al-Lazki, and M. Barazangi (2004). Regional seismic wave propagation ( $L_g$  and  $S_n$ ) and  $P_n$  attenuation in the Arabian plate and surrounding regions, *Geophys. J. Int.* **157**, 775–795.
- Alsinawi, S., and H. A. A. Ghalib (1975). Historical seismicity of Iraq, *Bull. Seismol. Soc. Am.* **65**, no. 5, 541–547.
- Alsinawi, S. A. (2006). Seismicity, in *Geology of Iraq*, S. Z. Jassim and Goff J. C. (Editors), Dolin, Prague and Moravian Museum, Brno, Czech Republic, 341 pp.
- Ambraseys, N. N. (1978). The relocation of epicenters in Iran, *Geophys. J. Roy. Astron. Soc.* **53**, 117–121.
- Ambraseys, N. N. (2001). Reassessment of earthquakes, 1900–1999, in the eastern Mediterranean and the Middle East, *Geophys. J. Int.* **145**, 471–485.
- Ambraseys, N. N. (2009). *Earthquakes in the Mediterranean and the Middle East: A Multidisciplinary Study of Seismicity up to 1900*, Cambridge University Press, Cambridge, England, 947 pp.
- Ambraseys, N. N., and J. A. Jackson (1998). Faulting associated with historical and recent earthquakes in the eastern Mediterranean region, *Geophys. J. Int.* **133**, no. 2, 390–406.
- Ambraseys, N. N., and C. P. Melville (1982). *A History of Persian Earthquakes*, Cambridge University Press, Cambridge, England, 219 pp.
- Boyd, O. S. (2012). Including foreshocks and aftershocks in time-independent probabilistic seismic-hazard analyses, *Bull. Seismol. Soc. Am.* **102**, no. 3, 909–917, doi: [10.1785/0120110008](https://doi.org/10.1785/0120110008).
- Castellaro, S., F. Mulargia, and Y. Y. Kagan (2006). Regression problems for magnitudes, *Geophys. J. Int.* **165**, 913–930.
- Covellone, B., and B. Savage (2012). A quantitative comparison between 1D and 3D source inversion methodologies: Application to the Middle East, *Bull. Seismol. Soc. Am.* **102**, no. 5, 2189–2199.
- Deniz, A., and M. S. Yucemen (2010). Magnitude conversion problem for the Turkish earthquake data, *Nat. Hazards* **55**, 333–352.
- Eken, T., K. Mayeda, A. Hofstetter, R. Gök, G. Örgülü, and N. Türkelli (2004). An application of the coda methodology for moment-rate spectra using broadband stations in Turkey, *Geophys. Res. Lett.* **31**, L11609, doi: [10.1029/2004GL019627](https://doi.org/10.1029/2004GL019627).
- Engdahl, E. R., and A. Villaseñor (2002). Global seismicity: 1900–1999, in *International Handbook of Earthquake Engineering and Seismology, Part A*, W. H. K. Lee, H. Kanamori, P. C. Jennings, and C. Kisslinger (Editors), chap. 41, Academic Press, London, England, 665–690.
- Fahmi, K. J., and J. N. Al Abbasi (1989). Some statistical aspects of earthquake occurrence in Iraq, *Earthq. Spectra* **5**, no. 4, 735–765.
- Fouad, S. F. A., and V. K. Sissakian (2011). Tectonic and structural evolution of the Mesopotamia Plain, special issue, *Iraqi Bull. Geol. Min.* **4**, 33–46.
- Gardner, J. K., and L. Knopoff (1974). Is the sequence of earthquakes in Southern California, with aftershocks removed, Poissonian?, *Bull. Seismol. Soc. Am.* **64**, 1363–1367.
- Giardini, D., G. Grunthal, K. M. Shedlock, and P. Zhang (1999). The GSHAP global seismic hazard map, *Ann. Geofisc.* **42**, no. 6, 1225–1230.
- Gök, R., L. Hutchings, K. Mayeda, and D. Kalafat (2009). Source parameters for 1999 for north Anatolian fault zone aftershocks, *Pure Appl. Geophys.* **166**, 547–566.
- Gök, R., A. Kaviani, E. M. Matzel, M. E. Pasyanos, K. Mayeda, G. Yertirmishli, I. El-Hussain, A. Al-Amri, F. Al-Jeri, T. Godoladze, et al. (2016). Moment magnitudes of local/regional events from 1D coda calibrations in the broader Middle East region, *Bull. Seismol. Soc. Am.* **106**, no. 5, 1926–1938, doi: [10.1785/0120160045](https://doi.org/10.1785/0120160045).
- Gök, R., H. Mahdi, H. Al-Shukri, and A. J. Rodgers (2008). Crustal structure of Iraq from receiver functions and surface wave dispersion: Implications for understanding the deformation history of the Arabian–Eurasian collision, *Geophys. J. Int.* **172**, 1179–1187.
- Gritto, R., M. S. Sibol, J. E. Siegel, H. A. Ghalib, Y. Chen, R. B. Herrmann, G. I. Alequabi, H. Tkalčić, B. S. Ali, B. I. Saleh, et al. (2008). Crustal structure of north Iraq from receiver function analysis, *2008 Monitoring Research Review: Ground-Based Nuclear Explosion Monitoring Technologies*, sponsored by Air Force Research Laboratory, 8 pp.
- Hainzl, S., F. Scherbaum, and C. Beauval (2006). Estimating background activity based on interevent-time distribution, *Bull. Seismol. Soc. Am.* **96**, no. 1, 313–320, doi: [10.1785/0120050053](https://doi.org/10.1785/0120050053).
- Hessami, K., and F. Jamali (2006). Explanatory notes to the map of major active faults of Iran, *J. Seismol. Earthq. Eng.* **8**, no. 1, 1–11.
- Jackson, J. A., T. J. Fitch, and D. P. McKenzie (1981). Active thrusting and the evolution of the Zagros Fold Belt, in *Thrust and Nappe Tectonics*, K. McClay and N. J. Price (Editors), Vol. 9, Geol. Soc. Lond. Spec. Publ., England, 371–379.
- Kanamori, H. (1977). The energy release in great earthquakes, *J. Geophys. Res.* **82**, no. 20, 2981–2987, doi: [10.1029/JB082i020p02981](https://doi.org/10.1029/JB082i020p02981).
- Kendall, M. G., and A. Stuart (1979). *The Advanced Theory of Statistics*, Fourth Ed., Vol. 2, Charles Griffin & Co. Ltd., London, United Kingdom, 758 pp.
- Marzocchi, W., and M. Taroni (2014). Some thoughts on declustering in probabilistic seismic-hazard analysis, *Bull. Seismol. Soc. Am.* **104**, 1838–1845.
- Mayeda, K., A. Hofstetter, J. L. O’Boyle, and W. R. Walter (2003). Stable and transportable regional magnitudes based on coda-derived moment-rate spectra, *Bull. Seismol. Soc. Am.* **93**, 224–239.
- Morasca, P., K. Mayeda, R. Gök, L. Malagnini, and C. Eva (2005). A break in self-similarity in the Lunigiana-Garfagnana region (northern Apennines), *Geophys. Res. Lett.* **32**, L22301, doi: [10.1029/2005GL024443](https://doi.org/10.1029/2005GL024443).
- Numan, N. M. S. (1997). A plate tectonic scenario for the Phanerozoic succession in Iraq, *Iraqi Geol. J.* **30**, no. 2, 85–119.
- Numan, N. M. S., R. A. Hammoudi, and J. Chorowicz (1998). Synsedimentary tectonics in the Eocene Pila Spi limestone formation in northern Iraq and its geodynamic implications, *J. Afr. Earth Sci.* **27**, no. 1, 141–148.
- Poirier, J. P., and M. A. Taher (1980). Historical seismicity in the near and Middle East, North Africa, and Spain from Arabic documents (VIIth–XVIIIth Century), *Bull. Seismol. Soc. Am.* **70**, no. 6, 2185–2201.
- Reasenber, P. (1985). Second-order moment of central California seismicity, 1969–1982, *J. Geophys. Res.* **90**, 5479–5495.
- Riad, S., and H. Meyers (1985). Earthquake catalog for the Middle East countries 1900–1983. *World Data Center for Solid Earth Geophysics Report SE-40*, National Oceanic and Atmospheric Administration (NOAA), US Department of Commerce, Boulder, Colorado.

- Richards, D. S. (2014). The annals of the Saljuq Turks: Selections from Al-Kamil Fi'l-Ta'rikh of Ibn Al-Athir, in *Routledge Studies in the History of Iran and Turkey*, Routledge, New York, New York, 320 pp.
- Sbeinati, M. R., R. Darawcheh, and M. Mouty (2005). The historical earthquakes of Syria: An analysis of large and moderate earthquakes from 1365 B.C. to 1900 A.D., *Ann. Geophys.* **48**, no. 3, 347–435.
- Shebalin, N. V., and R. E. Tatevossian (1997). Catalogue of large historical earthquakes of the Caucasus, in *Historical and Prehistorical Earthquakes in the Caucasus*, D. Giardini and S. Balassanian (Editors), NATO ASI Series 2: Environment, Vol. 28, Kluwer Academic Publishers, Dordrecht, The Netherlands, 201–232.
- Sissakian, V. K. (2013). Geological evolution of the Iraqi Mesopotamia foredeep, inner platform and near surroundings of the Arabian plate, *J. Asian Earth Sci.* **72**, 152–163.
- Zare, M., H. Amini, P. Yazdi, K. Sesetyan, M. B. Demircioglu, D. Kalafat, M. Erdik, D. Giardini, M. A. Khan, and N. Tsereteli (2014). Recent developments of the Middle East catalog, *J. Seismol.* **18**, 749–772.
- Zhuang, J., Y. Ogata, and D. Vere-Jones (2002). Stochastic declustering of space-time earthquake occurrences, *J. Am. Stat. Assoc.* **97**, 369–380.

*Tuna Onur*  
*Onur Seemann Consulting*  
*3378 Kingsley Place*  
*Victoria, British Columbia*  
*Canada V8P 4K1*  
*tuna@onurseemann.com*

*Rengin Gök*  
*Lawrence Livermore National Laboratory*  
*7000 East Avenue L-049*  
*Livermore, California 94550 U.S.A.*

*Wathiq Abdulnaby*  
*Seismological Laboratory, Department of Geology, College of*  
*Sciences*

*University of Basrah*  
*Basrah, Iraq*

*Hanan Mahdi*  
*Haydar Al-Shukri*  
*Graduate Institute of Technology*  
*University of Arkansas at Little Rock*  
*2801 South University Avenue*  
*Little Rock, Arkansas 72204 U.S.A.*

*Nazar M. S. Numan*  
*Department of Applied Geosciences*  
*University of Dubok*  
*Kurdistan Region, Iraq*

*Ammar M. Shakir*  
*Najah A. Abd*  
*University of Baghdad*  
*Department of Earth Sciences*  
*Baghdad, Al-Jadriya, Iraq*

*Hussein K. Chlaib*  
*Department of Soil Sciences and Water Resources*  
*University of Sumer*  
*Thi Qar Governorate, Iraq*

*Taber H. Ameen*  
*Geology Department/School of Science*  
*University of Sulaimani*  
*Sulaimani-Kerkuk Road, Sulaimaniyah*  
*Kurdistan Region, Iraq*

Published Online 29 March 2017